Structures along the Catalytic Pathway of PrmC/HemK, an N^5-Glutamine AdoMet-Dependent Methyltransferase†

Heidi L. Schubert,*,‡ John D. Phillips,§ and Christopher P. Hill‡

Departments of Biochemistry and of Medicine, University of Utah, Salt Lake City, Utah 84132

Received January 8, 2003; Revised Manuscript Received March 6, 2003

ABSTRACT: Posttranslational methylation of release factors on the glutamine residue of a conserved GGQ motif is required for efficient termination of protein synthesis. This methylation is performed by an N^5-glutamine methyltransferase called PrmC/HemK, whose crystal structure we report here at 2.2 Å resolution. The electron density at the active site appears to contain a mixture of the substrates, *S*-adenosyl-L-methionine (AdoMet) and glutamine, and the products, *S*-adenosyl-L-homocysteine (AdoHcy) and N^5-methylglutamine. The C-terminal domain of PrmC adopts the canonical AdoMet-dependent methyltransferase fold and shares structural similarity with the nucleotide *N*-methyltransferases in the active site, including use of a conserved (D/N)PPY motif to select and position the glutamine substrate. Residues of the PrmC ^{197}NPPY^{200} motif form hydrogen bonds that position the planar Gln side chain such that the lone-pair electrons on the nitrogen nucleophile are oriented toward the methyl group of AdoMet. In the product complex, the methyl group remains pointing toward the sulfur, consistent with either an sp^3-hybridized, positively charged Gln nitrogen, or a neutral sp^2-hybridized nitrogen in a strained conformation. Due to steric overlap within the active site, proton loss and formation of the neutral planar methylamide product are likely to occur during or after product release. These structures, therefore, represent intermediates along the catalytic pathway of PrmC and show how the (D/N)PPY motif can be used to select a wide variety substrates.

Posttranslational protein methylation of various amino acids is involved in a wide range of cellular processes, including RNA transport and processing (arginine), chemotaxis (glutamate), phycobilisome light-harvesting of complex proteins (asparagine), protein repair (L-isoaspartate), and chromatin regulation (lysine) (*1*−*5*). Methylation can function as a reversible signal, as in the case of the bacterial chemotaxis receptor, where glutamate residues are reversibly methylated to activate or attenuate an external signal (*2*), or as a more permanent modification that affects the activity or surface hydrophobicity of a substrate. Recent biochemical evidence has revealed that protein glutamine methylation is required to obtain efficient termination of protein translation (*6*, *7*).

During protein synthesis, the growing polypeptide chain extends from the P-site tRNA on the ribosome and remains covalently attached until a stop codon in the mRNA enters the A-site (*8*). Class-1 release factors (RFs[1]) recognize the stop codon and trigger peptide release by stimulating hydrolysis at the peptidyl transferase active site. A second class of RFs is then required to remove the class-1 RFs and begin disassembling the ribosome for a subsequent round of translation. Prokaryotic and eukaryotic class-1 release factors are structurally distinct and contain subfamilies of enzymes that are selective in their recognition of particular stop codons (*9*). Despite these differences, each class-1 RF contains a conserved GGQ motif that is thought to play a role in activating or positioning the water molecule involved in hydrolysis at the peptidyl transferase active site (*10*, *11*).

The release factor GGQ motif was initially identified as a crucial component of translation termination when mutation of either glycine residue resulted in a loss of termination in vitro despite continued interactions between the release factors and the ribosome (*11*). Peptide fragments containing the GGQ motif of active RF1 and RF2 from *Escherichia coli* were shown to contain a methylated glutamine by mass spectrometric analysis (*6*, *7*, *12*). Methylation of the N^5-nitrogen of glutamine is carried out by an AdoMet-dependent *N*-methyltransferase (N-MTase) encoded by a gene known as *hemK* (*7*, *12*, *13*), which was initially misidentified as a component of the heme biosynthetic pathway (*14*). The methylation is crucial for efficient translation termination, as shown by in vitro assays (*6*). *E. coli* strains containing a *hemK* knockout exhibit severely retarded growth, increased stop codon read-through, and an induction of the oxidative stress response (*7*, *12*). A similar phenotype is observed when the release factor is overproduced, overwhelming the MTase and remaining largely unmethylated and inactive (*6*). A *hemK* family member is also found in higher eukaryotes, including

† Funding was received from NIH grants GM56775 and KO1 DK02794.

* Address correspondence to this author at 1900 East, 20 North, Rm. 211, Department of Biochemistry, University of Utah, Salt Lake City, UT 84132-3201. Phone: (801) 585-3919. Fax: (801) 581-7959. E-mail: heidi@biochem.utah.edu.

‡ Department of Biochemistry.

§ Department of Medicine.

[1] Abbreviations: *S*-adenosyl-L-methionine, AdoMet; *S*-adenosyl-L-homocysteine, AdoHcy; multiple anomalous diffraction, MAD; methyltransferase, MTase; Release factor, RF; glutamine, Gln; N^5-methylglutamine, MeGln; Protein Data Bank, PDB.

10.1021/bi034026p CCC: $25.00
Published on Web 04/19/2003

human, and mammalian release factors also contain the GGQ motif, suggesting that methylation on glutamine is a universal requirement for peptide termination. It has been suggested that the *hemK* gene name should be replaced with *prmC* to reflect the role of these homologues in the greater field of *p*rotein *r*ibosomal *m*ethylation, or perhaps more accurately, *p*rotein *r*elease factor *m*ethylation (*7*). For this work, we will refer to the purified enzyme as PrmC.

S-Adenosyl-L-methionine (AdoMet) is the second most widely used cofactor after ATP, and its methyl group is transferred to a wide variety of substrates, including DNA, RNA, small molecules, and amino acids, to generate *S*-adenosyl-L-homocysteine (AdoHcy) and a methylated product. The most prevalent architecture of the AdoMet-dependent MTases is a mixed α/β-domain containing a seven-stranded β-sheet that provides both the AdoMet binding pocket and the base of the active site (*15*, *16*). The (N/D)PPY motif found at the end of β4 in adenosine and cytosine N-MTases is crucial in positioning the nucleotide substrate (*17*). The structure of the adenosine N-MTase, *Taq*I, bound to DNA revealed that the N^6-adenine nitrogen donates hydrogen bonds to the (D/N)PPY motif, which forms a semicircle around the substrate, essentially in the plane of the nucleotide (*18*). These interactions have been postulated to position the nucleophile such that the lone-pair electrons are directed toward the incoming methyl group (*17*−*19*).

In an effort to understand how the (N/D)PPY motif of PrmC facilitates methylation on the N^5-nitrogen of glutamine, as opposed to adenine, we have determined the structure of the *Thermotoga maritima* PrmC bound to a partial occupancy mixture of substrates, AdoMet and glutamine, and products, AdoHcy and a N^5-methylglutamine (MeGln); the transferred methyl group was refined at half-occupancy on both the AdoMet and MeGln molecules. We also report the 2.35 Å resolution structure of an AdoHcy-bound PrmC in a different crystal form. PrmC adopts the canonical AdoMet-dependent MTase fold and employs the NPPY motif to bind the planar glutamine amide through interactions similar to those made by N-MTases that act on nucleotide ligands. The methyl group in the MeGln points toward the AdoHcy and in a direction perpendicular to the plane of the glutamine side-chain amide, consistent with a charged sp^3-hybridized nitrogen or a strained neutral sp^2-hybidized nitrogen. It appears that steric hindrance ensures that the planar MeGln product can be obtained only after product release from the active site. The structure also reveals that PrmC exhibits a negatively charged substrate binding cleft that is complementary to the positively charged loops of the release factors that contain the GGQ motif.

EXPERIMENTAL PROCEDURES

Expression, Purification, and Crystallization. The *prmC*/*hemK* gene was amplified from *T. maritima* genomic DNA using two primers: forward, 5′-CAACGTGGAGGTGGAGCTCAC-3′, and reverse, 5′-GGAGAAGTTAGACTGATACTC-3′. The clone was ligated into pGEM-Easy (Promega) and was shown to have a sequence identical with that of Genbank accession number NP_228298. The gene was cleaved with *Nco*I−*Pvu*II, and subcloned into pHIS-.Parrallel3 (*20*) cleaved with *Nco*I−*Stu*I. The vector contained an N-terminal His tag and a TEV protease cleavage site. Bacterial cultures were grown and induced using standard protocols. Initial protein purification was carried out by affinity chromatography using Pharmacia chelating sepharose charged with Ni^{2+} and standard protocols. Fractions were dialyzed against 20 mM Tris-HCl, 100 mM NaCl, and 1 mM DTT, pH 8.0, and concentrated. The His tag was removed by recombinant His-tagged TEV protease, PrmC:TEV 1:50, at room temperature for 2 h. The cleaved protein was dialyzed a second time to remove the DTT and separated from the tag and TEV by repeating the Ni^{2+} chromatography. Finally, the cleaved protein was concentrated and run on a Pharmacia S75 gel filtration column equilibrated in the dialysis buffer. PrmC eluted at a volume consistent with a monomeric state.

PrmC was crystallized at 19 °C in hanging drops by mixing 2 μL of PrmC solution at 14 mg/mL with an equal volume of the well solution [16−20% poly(ethylene glycol) (MW 3000) and 100 mM sodium citrate trihydrate, pH 5.5]. Crystals grew as flat plates. In the absence of ligand, the crystals belong to space group $P2_12_12$ and contain one molecule per asymmetric unit bound to AdoHcy. Enzyme that was preincubated with 5 mM AdoMet and glutamine prior to crystallization produced morphologically similar crystals that belonged to space group *C*2, had two molecules per asymmetric unit, and bound a mixture of AdoMet/Gln and AdoHcy/MeGln in the active site. This crystal form was also obtained using selenomethionine-substituted PrmC that was produced using the methionine inhibition method (*21*); selenomethionine incorporation was confirmed by amino acid analysis.

Data Collection and Model Refinement. For data collection, both crystal forms were cryoprotected in the well condition made up with 20% glycerol and cooled by plunging into liquid nitrogen. Native *C*2 data to 2.2 Å and selenium multiple anomalous diffraction (MAD) data to 2.7 Å resolution were collected at the Stanford Synchrotron Radiation Laboratory (SSRL) beamline 9-2 (Table 1). The $P2_12_12$ data set was collected to 2.35 Å resolution on SSRL beamline 9-1. All data were processed and scaled using the HKL set of programs (Table 1) (*22*). Three pairs of selenomethionine sites were identified and phased using the program SOLVE (*23*). In addition, the sulfur atoms of the bound AdoMets gave the next-highest anomalous difference peaks and were used for phasing, suggesting that some selenomethionine had been converted into AdoMet during bacterial production and that not all of the bound AdoMet/AdoHcy came from the precrystallization incubation. The phases were refined by solvent flattening, and a preliminary polyalanine trace was obtained using the program RESOLVE (*24*). Further model building and refinement were performed with the programs "O" (*25*) and REFMAC5 (*26*).

The final model in the *C*2 space group contains residues 12−282 of molecule A and residues 14−52 and 56−281 of molecule B. Each monomer contains an AdoMet/AdoHcy mixture where the catalytic methyl is modeled at half-occupancy. In addition, a MeGln product has been modeled into the active site, with the methyl group refined at half-occupancy. The active site of molecule B has electron density consistent with the density in molecule A, but due to weak data only the tips of the side chains were refined. The dictionary library for the MeGln was created by the sketcher program within the CCP4 suite of programs (*27*). The structure of the $P2_12_12$ crystal form was determined by

Table 1. Crystallographic Statistics

data collection statistics	high res	Se-peak	Se-remote	Se-inflect.	$P2_12_12$
space group	*C*2	*C*2	*C*2	*C*2	$P2_12_12$
a (Å)	141.5	141.3	141.8	141.8	63.8
b (Å)	59.1	58.7	59.1	59.1	59.0
c (Å)	85.6	84.5	85.2	85.2	82.9
β (deg)	109.2	109.0	109.4	109.4	
wavelength (Å)	1.033	0.97884	0.95369	0.97900	0.97
resolution (Å)[a]	20−2.2 (2.28−2.2)	20−2.7 (2.8−2.7)	20−2.7 (2.8−2.7)	20−2.7 (2.8−2.7)	20−2.35 (2.43−2.35)
no. of observed reflections	176 619	63 308	63 775	64 390	100 547
no. of unique reflections	32 346	18 102	18 098	18 207	24 661
% completeness[a]	94.7 (66.5)	97.3 (89.0)	97.9 (92.7)	99.1 (95.5)	97.7 (79.4)
R-merge[a,b]	5.0 (35.1)	6.1 (19.0)	5.9 (18.6)	7.2 (24.6)	3.9 (40.4)
$I/\sigma I$	26.3 (2)	9.8 (3.3)	10.3(3.3)	12.3 (3.6)	20.0 (2.3)
mosaicity (deg)	0.95	1.35	1.29	1.24	0.5
R-factor[c]	19.2				23.8
R_{free}[d]	25.4				30.0
rmsd (bond lengths) (Å)	0.020				0.026
rmsd (bond angles) (deg)	1.8				2.6

[a] Numbers in parentheses are for the high-resolution bin. [b] *R*-merge $= \sum|\bar{I}|/\sum I$, where I is the intensity of an individual measurement and $\bar{I}$ is the average intensity from multiple observations. [c] *R*-factor $= \sum||F_{obs}| - k|F_{calc}||/\sum|F_{obs}|$. [d] R_{free} equals the *R*-factor against 5% of the data removed prior to refinement.

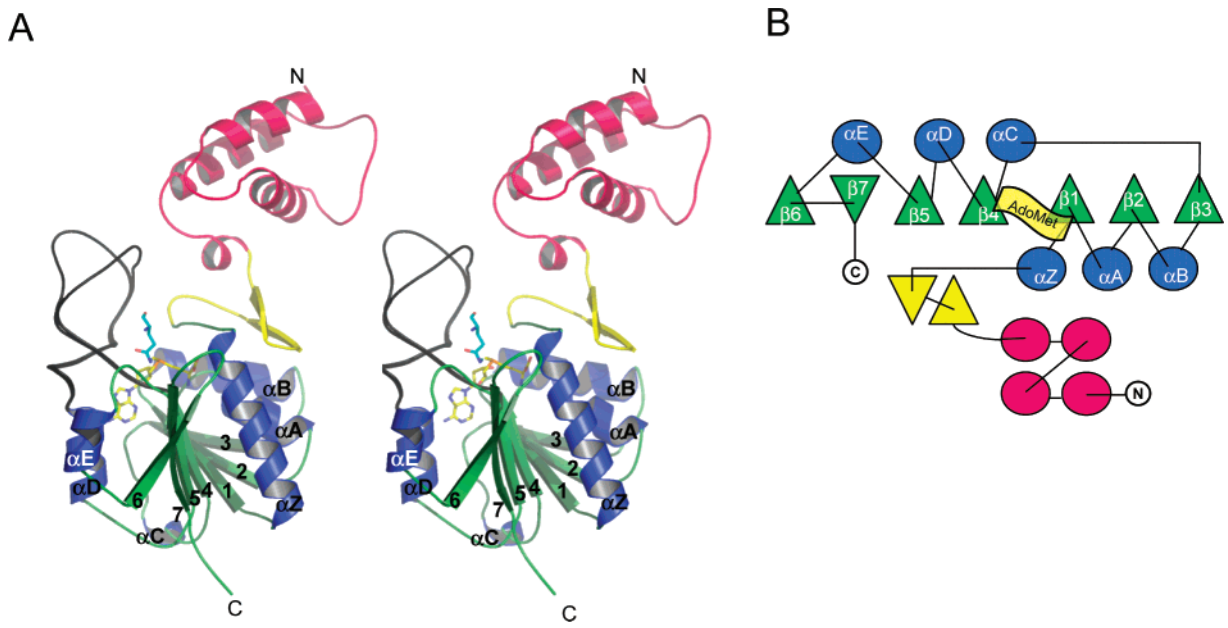

FIGURE 1: Structure of PrmC. (A) Stereodiagram of the enzyme with the N-terminal helical domain colored magenta, the *β*-hairpin subdomain colored yellow, and the catalytic domain colored with blue helices and green strands. The bound AdoMet (yellow) and methylglutamine (cyan) delineate the active site. In the three independently determined PrmC molecules, the *β*4−αD loop (shown in black) adopts two alternate conformations (both shown) and is not visible in the third. [Figures 1A, 2B, 3, 4, and 6A−D were prepared using the program Pymol (*40*).] (B) Topology diagram.

molecular replacement using the *C*2 PrmC model and refined independently. The final refined model contains residues 13−205, 212−282, and an AdoHcy molecule that was retained throughout purification. Both structures have been submitted to the Protein Data Bank (PDB) with accession codes 1NV8 and 1NV9 for the *C*2 and $P2_12_12$ data, respectively. See Table 1 for data collection and refinement statistics.

RESULTS

Structure of PrmC. The crystal structure of *T. maritima* PrmC was determined by MAD phasing using selenomethionine-substituted protein. Data were collected to 2.2 Å resolution from a *C*2 crystal containing two molecules per asymmetric unit, and to 2.35 Å resolution from a $P2_12_12$ crystal containing a single molecule in the asymmetric unit. The *C*2 and $P2_12_12$ structures have been refined to final *R*-factors of 19.2% (R_{free} = 25.4%) and 23.9% (R_{free} = 30.0%), respectively, with reasonable geometry (Table 1). The structures of the three crystallographically independent molecules are essentially identical, with rms deviations between 0.31 and 0.52 Å over all Cα carbons.

PrmC assembles into two major domains: an N-terminal domain consisting of four α-helices is connected to the larger AdoMet binding domain through a small *β*-hairpin (Figure 1). Similar to other AdoMet-dependent MTases, the catalytic domain is comprised of a seven-stranded mixed *β*-sheet flanked by six α-helices. This domain is most similar to the structures of *Methanococcus jannaschii* mj0882 (PDB code 1DUS), *Mycobacterium tuberculosis* rv2118c (PDB code 1I9G), the catechol O-MTase (PDB code 1VID), and the glycine O-MTase (PDB code 1XVA). These four structures share only 10−21% sequence identity with PrmC, although

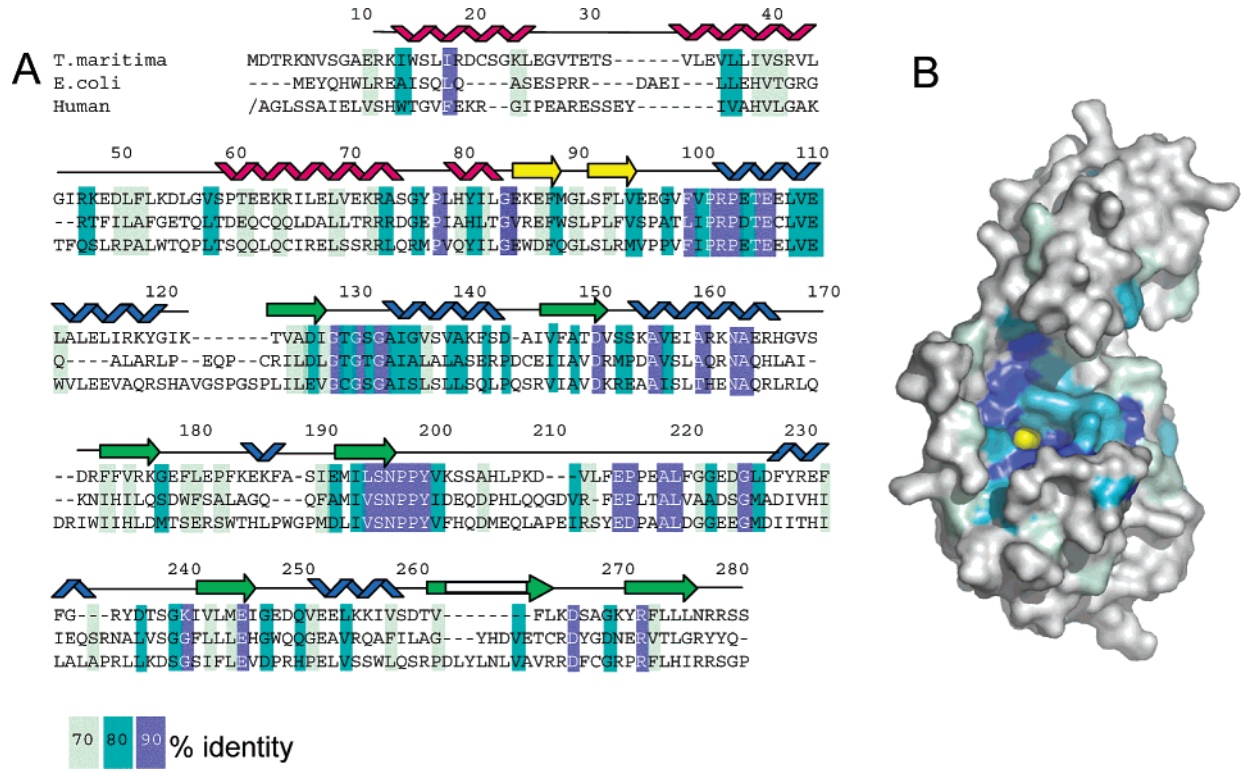

FIGURE 2: Conservation of PrmC. (A) Sequence alignment of PrmC/HemK from *T. maritima*, *E. coli*, and human, colored according to the conservation in sequence between these and 15 additional PrmC/HemK family members, including *Neisseria meningitidis* MC58, *Aquifex aeolicus*, *Buchnera* sp. APS, *Chlamydia trachomatis*, *Bacillus halodurans*, *Xylella fastidiosa*, *Haemophilus influenzae*, *Rickettsia prowazekii*, *Bacillus subtilis*, *Mycobacterium tuberculosis*, *Deinococcus radiodurans*, *Synechocystis* PCC6803, *Bacillus halodurans*, *Helicobacter pylori* (strain 26695), and *Porphyromonas gingivalis*. The highlighted conservation ranges from 90% identical between all 14 sequences, in blue, down to 70% identical, in light green. The *T. maritima* numbering and secondary structure are shown above the sequence. (B) The surface of PrmC colored by sequence conservation and in the same orientation as in Figure 1A. The bound AdoMet molecule is colored in yellow at the bottom of the active site cleft (no Gln or MeGln is shown in this figure).

the *Z*-scores for structural similarity, as defined by the DALI structural comparison server (*28*), range from 11 to 18, where a *Z* score greater than 2 indicates significant structural similarity. Despite their similarity, the PrmC and *Me. jannaschii* mj0882 enzyme families probably have distinct substrates, and mj0882 has been putatively labeled as an RNA:(guanine-N^2) MTase (*29*). The majority of the similarity to other MTases is contained within the AdoMet binding domain, and an alignment of 14 members of the PrmC/HemK family revealed 15 invariant residues (Figure 2). The *T. maritima* PrmC sequence shares 31% identity (51% similarity) with the extensively studied *E. coli* enzyme. The N-terminal domain of PrmC does not exhibit statistically significant similarity with any other MTase. It is located above the active site (Figure 1) and, as shown for the variable auxiliary domains of other MTases (*18*, *30*), may contribute to binding of the protein substrate.

AdoMet Binding within the Active Site. All three crystallographically independent PrmC structures presented here contain some form of AdoMet or AdoHcy. The *C*2 crystal form apparently contains an approximately 50:50 mixture of AdoMet and AdoHcy bound to both molecules in the asymmetric unit (Figure 3), while the $P2_12_12$ crystal form contains only AdoHcy. In all cases, the methyl donor is bound above the β-sheet near the hallmark nucleotide binding sequence, GxGxG, at the C-terminal end of β1. As in other MTases, the AdoMet adenine ring packs against the hydrophobic side chains of Ile128, Val152, Phe180, and Phe228. Both hydroxyl groups of the ribose ring form hydrogen-bonding interactions with the conserved side chain of Asp151, and the methionine moiety interacts with Asn197, Gly129, and two water molecules. The nonpolar side chain of Phe100 packs behind the sulfur atom of AdoMet and may function to destabilize the charged ligand, thereby enhancing the rate of methylation.

Evolutionarily conserved residues (Figure 2) are concentrated at the active site cleft, which is a deep and narrow funnel (10 Å diameter opening × 8 Å deep) that leads to the reactive donor methyl, which is barely visible at the bottom of the pocket (yellow in Figure 2B). One side of this funnel is lined with the hydrophobic residues Tyr200, Val201, Leu219, and Phe100, while the other side is lined with charged residues Arg103, Glu105, Glu246, Glu249, and Arg273. Additional negatively charged amino acids lace the surface of PrmC surrounding the active site and generate an overall electronegative surface (Figure 6E). The bottom of the active site is formed by the conserved NPPY motif, positioned at the end of β4, and centered on a sharp kink on the polypeptide chain. Recognition of this motif within PrmC prompted an earlier incorrect designation as an adenosine methyltransferase, because this motif is a hallmark of the active site of the adenosine and cytosine N-MTases (*17*, *31*). Indeed, the NPPY motif in PrmC adopts a conformation very similar to that in *Taq*I, and in both cares these residues are crucial for substrate recognition and selectivity.

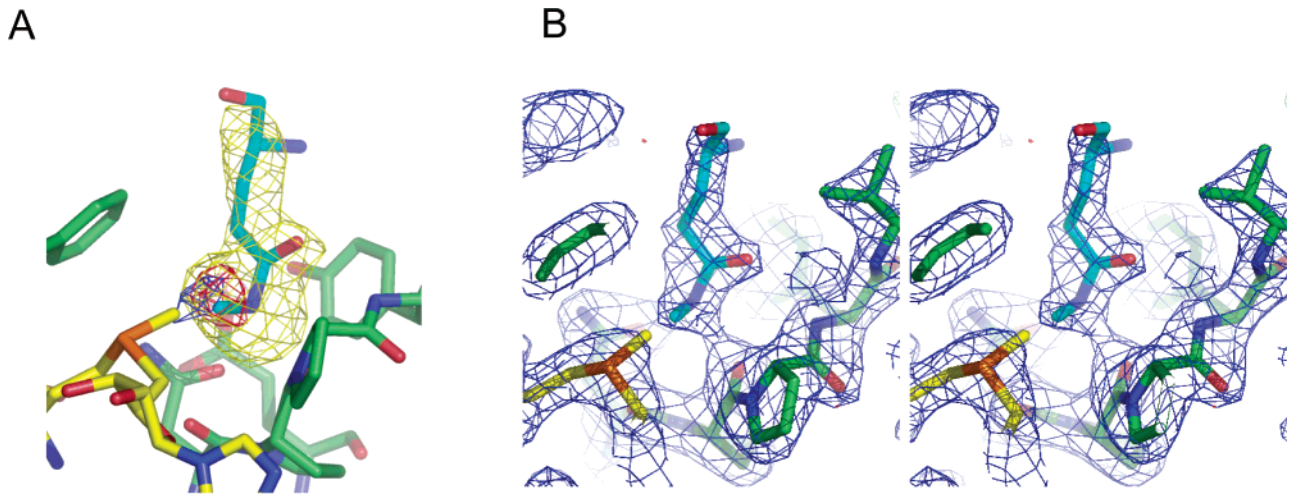

FIGURE 3: Electron density surrounding the active sites of the *C*2 crystal form. (A) The final model containing a mixture of two catalytic intermediates Gln and MeGln(cyan) is shown bound to the active site residues (green) near the AdoMet/AdoHcy cofactor (yellow). $F_o - F_c$ map calculated during refinement prior to addition of the Gln/MeGln residue to the model (3σ, yellow). $F_o - F_c$ map (3σ, red) calculated following refinement of MeGln (Me occupancy = 0) and AdoMet (Me occupancy = 0.5) supports the presence of a methyl group on the Gln nitrogen. Conversely, an $F_o - F_c$ map (3σ, blue) following refinement of MeGln (Me occupancy = 0.5) and AdoMet (Me occupancy = 0) supports the refinement of partial occupancy of the AdoMet methyl group. (B) $2F_o - F_c$ (1σ, blue) electron density reflects the quality of data and refinement.

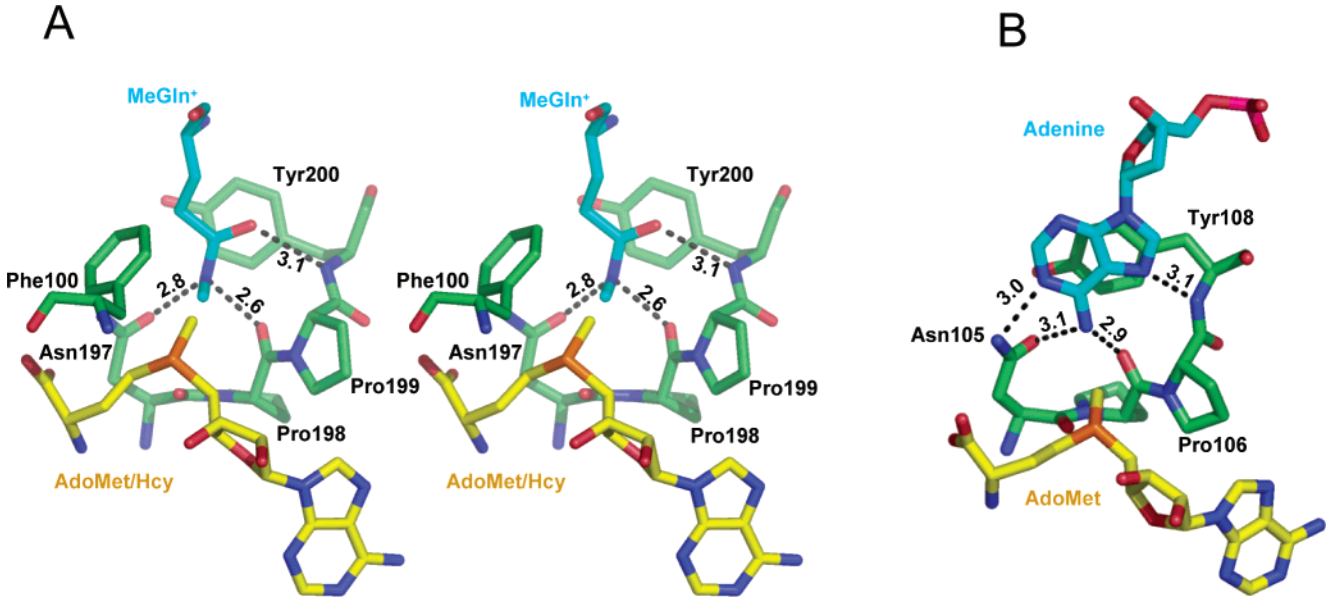

FIGURE 4: Active site of PrmC and comparison to *Taq*I. (A) Stereoview of the PrmC active site. Hydrogen-bonding interactions between the Gln/MeGln (cyan) and the enzyme are shown as dashed lines, with distances in angstroms noted. The distance between the Gln nitrogen nucleophile and the methyl donor on AdoMet is 3.3 Å. (B) Structure of the adenosine N-MTase *Taq*I bound to AdoMet and adenosine. A substrate-bound *Taq*I model was generated by alignment of the *Taq*I AdoMet-bound structure (PDB code 2ADM) (*41*) with the *Taq*I adenosine-bound structure (PDB code 1G38) (*18*) [using residues immediately surrounding the active site and the (D/N)PPY motif, residues 46−50 and 104−108]. The donor methyl group is 3.0 Å from the N^6-nitrogen in this model.

A Combination of Substrates and Products Are Bound to the Active Site. The *C*2 crystal form, which was grown in the presence of 5 mM AdoMet and glutamine, contains electron density in the active site that was initially interpreted as being due to a Gln side chain. Following preliminary refinement, residual density (Figure 3) suggested that the methyl group was partially present on both the AdoMet and the Gln nitrogen atom, indicative of partial turnover of substrates to products. Refinement proceeded smoothly and gave flat difference density maps when the model was treated as a mixture of substrates and products, with the methyl group of the MeGln ligand, and the AdoMet methyl group, modeled with half-occupancy.

Hydrogen-bonding interactions and positioning of the MeGln with respect to the NPPY motif explain the enzyme specificity. The N^5-nitrogen nucleophile of the Gln side chain is positioned within hydrogen-bonding distance of the carbonyl oxygen of Pro198 and the side-chain oxygen of Asn197 (Figure 4A), while the Gln side-chain oxygen accepts a hydrogen bond from the main-chain amide of Tyr200. The rest of the Gln residue does not make specific contacts with the enzyme, although the aromatic ring of Tyr200 packs against the side-chain methylene groups. The hydrogen bonds to the NPPY motif lie within the plane of the sp^2-hybridized nitrogen nucleophile, and the lone-pair electrons from the nitrogen would project perpendicular to that plane, pointing

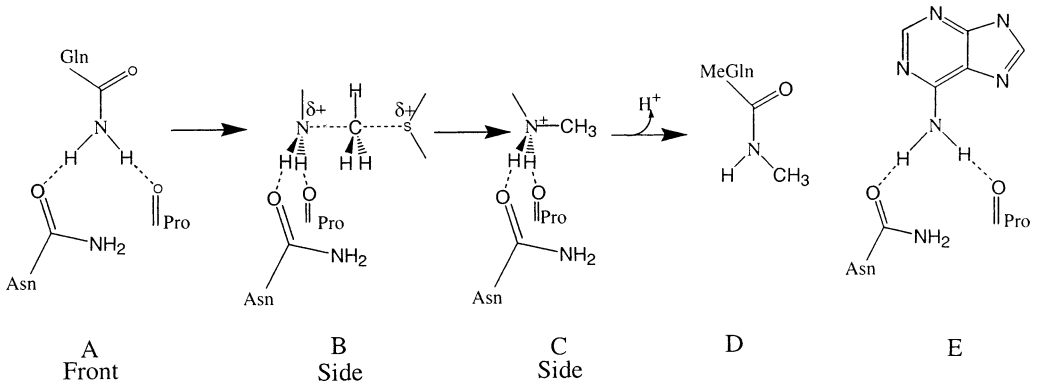

FIGURE 5: Proposed catalytic mechanism of (D/N)PPY-containing N-MTases. (A) The planar substrate is positioned by the conserved (D/N)PPY motif such that the lone pairs of the nucleophilic nitrogen point toward the incoming methyl group and the charged sulfonium ion. (B,C) Hydrogen bonds from the (D/N)PPY motif may help to position the lone-pair orbital. The reaction proceeds with inversion of symmetry surrounding the methyl group in a typical S_N2-type reaction to yield a charged sp^3-hybridized nitrogen center. (D) The final neutral product is obtained after proton loss to solvent. (E) Equivalent binding geometry is observed for the adenosine N-MTase, *Taq*I, which presumably utilizes a similar catalytic mechanism.

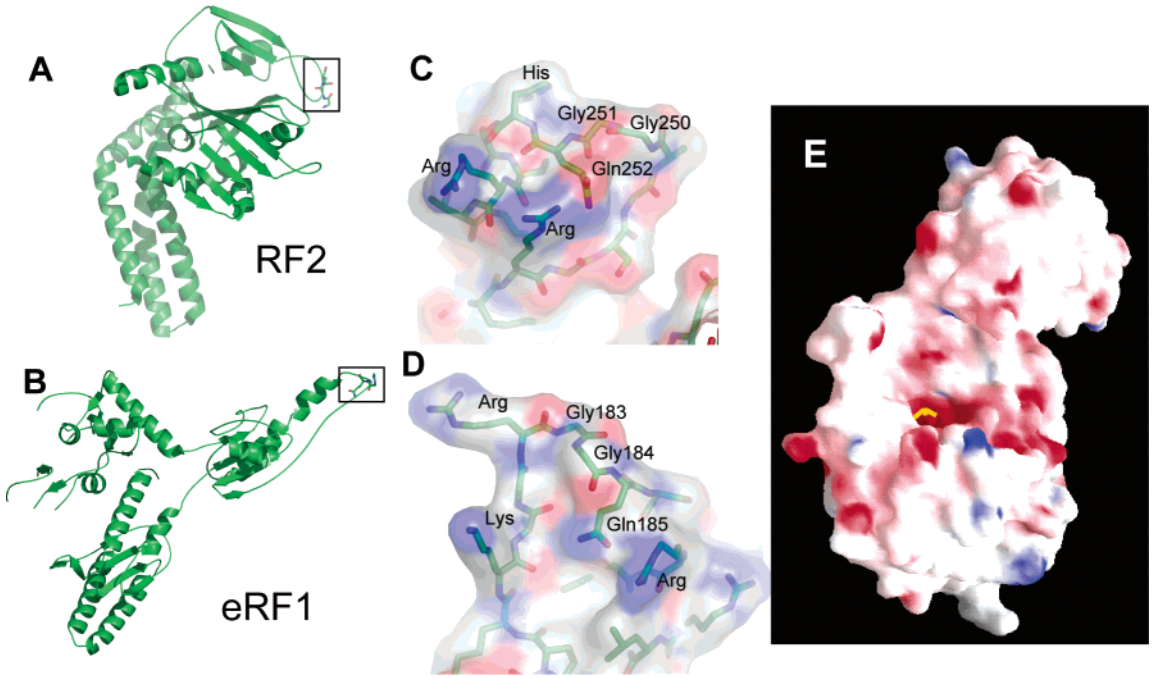

FIGURE 6: PrmC is reactive against the glutamine of the GGQ motif of peptide release factors. (A,B) The tertiary structure of RF2 (PDB code 1QGE) and eRF1 (PDB code 1DT9), with the GGQ motif highlighted in ball-and-stick representation and boxed. (C,D) The surface of the RF2 and eRF1 surface loops containing the GGQ motif and other nearby residues, colored by atom type: red, oxygen; blue, nitrogen; and white, carbon. (E) A surface representation of PrmC colored by electrostatic potential, indicating the strong negative charge of the active site (−22, −11, 0, +11, 22 eV).

toward the incoming methyl group (Figure 5A).

Transfer of the methyl from the AdoMet sulfur to the Gln nitrogen is thought to follow a classic S_N2 mechanism in which the symmetry of the methyl group is inverted (Figure 5B). This is consistent with the substrate and product complex structures seen here, which respectively show S−C−N angles of 156° and 161°, similar to the linear geometry of 180°. The short 3.3 Å distance seen between the Gln nitrogen and the AdoMet methyl in the substrate complex, and the 3.6 Å separation of the product complex $MeGln^+$ methyl and the AdoMet sulfur, are also consistent with a direct mechanism of methyl transfer.

The methyl group on the MeGln product points toward the AdoMet/AdoHcy sulfur, in a direction perpendicular to that expected for an sp^2-hybridized nitrogen. It seems possible, therefore, that the bound product is actually a methylated intermediate prior to the final step of deprotonation. This $MeGln^+$ species would contain an sp^3-hybridized nitrogen and retain the two hydrogen bonds to Asn197OD1 and Pro198O seen in the substrate complex (Figure 5C). Alternately, the MeGln species may have lost a proton to solution and may contain a neutral sp^2-hybridized nitrogen, albeit in a strained conformation (*32*). We suggest that the planar conformation is prohibited by steric overlap of the methyl group with Asn197 and Pro198, and that the final step of deprotonation could occur during or following product release. This model is also consistent with the apparent absence of a suitable general base or solvent molecule adjacent to the bound MeGln in the crystal structure.

Comparison with Other Methyltransferases. Like PrmC, *Taq*I binds the sp^2-hybridized NH_2 group of its substrate (adenine) by hydrogen bonds with the (D/N)PPY motif that

lie in the plane of the substrate (Figures 4B and 5E). In contrast, many AdoMet-dependent MTases do not contain the (D/N)PPY motif and have evolved alternate methods of substrate binding, nucleophilic activation, and proton abstraction. The cytidine C^5-MTase, *Hha*I, generates a covalent intermediate between a cysteine residue and the nucleotide's C^6-carbon to activate the C^5 position for nucleophilic attack on AdoMet (*33*, *34*). In the catechol O-MTase, a Mg^{2+} ion coordinates the substrate's hydroxyl groups and activates the hydroxyl nucleophile, and a lysine residue has been implicated in proton abstraction (*35*, *36*). The active site of the glutamate O-MTase, CheR, contains an arginine residue, and conversely, the active site of the arginine N-MTase, PRMT, contains multiple glutamate residues (*37*, *38*). Charge complementarity is therefore predicted to facilitate binding and positioning of substrate in these MTases, and proton abstraction is thought to require a nearby tyrosine (CheR) or histidine residue (PRMT) (*38*).

Interaction of PrmC with the Peptide Release Factors. The structures of eukaryotic eRF1 and prokaryotic RF2 (both class-1 RFs) share little similarity aside from the GGQ motif (Figure 6A,B), which is positioned within a surface loop (*10*, *39*). In both cases, the Gln residue is packed against the surface of the protein (Figure 6C,D), indicating that some conformational change, perhaps involving the flexible glycine residues, will be required in order to bind into the PrmC active site cleft. It has been observed that the region flanking the GGQ motif of both eRF1 and RF2 contains several basic residues, such as Arg, Lys, and His (Figure 6C,D) (*11*). A role for electrostatic interactions in substrate binding is therefore suggested by the negative potential surrounding the PrmC active site, which is due to both conserved acidic residues within the active site and several less conserved acidic residues on the surface of the enzyme (Figure 6E).

This hypothesis is supported by the predicted charge distribution on the surface of the *E. coli* ribosomal protein L3 Gln MTase YfcB/PrmB (*7*), which shares 32% sequence identity with *E. coli* PrmC including the NPPY motif. A simple molecular modeling experiment, in which the residues surrounding the PrmC active site were replaced with the corresponding PrmB residues, generates a model that is essentially identical to PrmC at the active site. The model reveals a substantial change in the electrostatic surface of the active site due to the replacement of three glutamates with nonacidic residues, Glu249-Asn, Glu104-Pro, and Glu107-Gly. This corresponds well with the lack of basic residues surrounding the site of glutamine methylation in L3 (*7*).

CONCLUSION

In summary, the structure of PrmC describes a new family of AdoMet-dependent enzymes that methylate Gln residues. This family was initially described as putative adenosine N-MTases due to the possession of a (D/N)PPY motif that we have now shown can bind the planar amide side chain of Gln, and presumably Asn, as well as the DNA nucleotides adenine and cytidine. We propose that all N-MTases containing the (D/N)PPY motif effect catalysis by precisely orienting the substrate for methyl transfer and promote product release by preventing the bound product from adopting the ground-state conformation. These results underscore the remarkable flexibility of the MTases, which possess a highly conserved AdoMet binding domain but have otherwise diverged greatly to bind widely disparate substrates and have developed several different mechanisms to activate substrate for methyl transfer from AdoMet.

REFERENCES

1. Gary, J. D., and Clarke, S. (1998) *Proc. Natl. Acad. Sci. U.S.A. 61*, 65−131.
2. Levit, M. N., and Stock, J. B. (2002) *J. Biol. Chem. 15*, 15.
3. Klotz, A. V., and Glazer, A. N. (1987) *J. Biol. Chem. 262*, 17350−17355.
4. Najbauer, J., Orpiszewski, J., and Aswad, D. W. (1996) *Biochemistry 35*, 5183−5190.
5. Lachner, M., and Jenuwein, T. (2002) *Curr. Opin. Cell Biol. 14*, 286−298.
6. Dincbas-Renqvist, V., Engstrom, A., Mora, L., Heurgue-Hamard, V., Buckingham, R., and Ehrenberg, M. (2000) *EMBO J. 19*, 6900−6907.
7. Heurgue-Hamard, V., Champ, S., Engstrom, A., Ehrenberg, M., and Buckingham, R. H. (2002) *EMBO J. 21*, 769−778.
8. Kisselev, L. L., and Buckingham, R. H. (2000) *Trends Biochem. Sci. 25*, 561−566.
9. Ehrenberg, M., and Tenson, T. (2002) *Nat. Struct. Biol. 9*, 85−87.
10. Song, H., Mugnier, P., Das, A. K., Webb, H. M., Evans, D. R., Tuite, M. F., Hemmings, B. A., and Barford, D. (2000) *Cell 100*, 311−321.
11. Frolova, L. Y., Tsivkovskii, R. Y., Sivolobova, G. F., Oparina, N. Y., Serpinsky, O. I., Blinov, V. M., Tatkov, S. I., and Kisselev, L. L. (1999) *RNA 5*, 1014−1020.
12. Nakahigashi, K., Kubo, N., Narita, S., Shimaoka, T., Goto, S., Oshima, T., Mori, H., Maeda, M., Wada, C., and Inokuchi, H. (2002) *Proc. Natl. Acad. Sci. U.S.A. 99*, 1473−1478.
13. Clarke, S. (2002) *Proc. Natl. Acad. Sci. U.S.A. 99*, 1104−1106.
14. Nakayashiki, T., Nishimura, K., and Inokuchi, H. (1995) *Gene 153*, 67−70.
15. Fauman, E. B., Blumenthal, R. M., and Cheng, X. (1999) in *S-Adenosylmethionine-dependent Methyltransferases: Structures and Functions* (Cheng, X., and Blumenthal, R. M., Eds.) pp 3−38, World Scientific Publishing, River Edge, NJ.
16. Martin, J. L., and McMillian, F. M. (2002) *Curr. Opin. Struct. Biol. 12*, 783−793.
17. Malone, T., Blumenthal, R. M., and Cheng, X. (1995) *J. Mol. Biol. 253*, 618−632.
18. Goedecke, K., Pignot, M., Goody, R. S., Scheidig, A. J., and Weinhold, E. (2001) *Nat. Struct. Biol. 8*, 121−125.
19. Newby, Z. E., Lau, E. Y., and Bruice, T. C. (2002) *Proc. Natl. Acad. Sci. U.S.A. 99*, 7922−7927.
20. Sheffield, P., Gerrard, S., and Derewenda, Z. (1999) *Protein Exp. Purifi. 15*, 34−39.
21. Van Duyne, G. D., Standaert, R. F., Karplus, P. A., Schreiber, S. L., and Clardy, J. (1993) *J. Mol. Biol. 229*, 105−124.
22. Otwinowski, Z., and Minor, W. (1997) *Methods Enzymol. 267*, 307−326.
23. Terwilliger, T. C. (2001) *Acta Crystallogr. D, Biol. Crystallogr. 57*, 1763−1775.
24. Terwilliger, T. C. (2001) *Acta Crystallogr. D, Biol. Crystallogr. 57*, 1755−1762.
25. Jones, A. T., Zou, J.-Y., Cowan, S. W., and Kjeldgaard, M. (1991) *Acta Crystallogr. D, Biol. Crystallogr. A47*, 110−119.
26. Murshudov, G. N., and Dodson, E. J. (1997) *Acta Crystallogr. D, Biol. Crystallogr. 53*, 240−255.
27. *Acta Crystallogr.* (1994) *D50*, 760−763.
28. Holm, L., and Sander, C. (1993) *J. Mol. Biol. 223*, 123−138.
29. Bujnicki, J. M., and Rychlewski, L. (2002) *BMC Bioinformatics 3*, 10.
30. Klimasauskas, S., Kumar, S., Roberts, R. J., and Cheng, X. (1994) *Cell 76*, 357−369.
31. Bujnicki, J. M., and Radlinska, M. (1999) *IUBMB Life 48*, 247−249.

32. Milner-White, E. J. (1997) *Protein Sci. 6*, 2477−2482.
33. Wu, J. C., and Santi, D. V. (1987) *J. Biol. Chem. 262*, 4778−4786.
34. Lau, E. Y., and Bruice, T. C. (1999) *J. Mol. Biol. 293*, 9−18.
35. Vidgren, J., Svensson, L. A., and Liljas, A. (1994) *Nature 368*, 354−357.
36. Zheng, Y.-J., and Bruice, T. C. (1997) *J. Am. Chem. Soc. 119*, 8137−8145.
37. Djordjevic, S., and Stock, A. M. (1997) *Structure 5*, 545−558.
38. Zhang, X., Zhou, L., and Cheng, X. (2000) *EMBO J. 19*, 3509−3519.
39. Vestergaard, B., Van, L. B., Andersen, G. R., Nyborg, J., Buckingham, R. H., and Kjeldgaard, M. (2001) *Mol. Cell 8*, 1375−1382.
40. DeLano, W. L. (2002) http://www/pymol.org.
41. Schluckebier, G., Kozak, M., Bleimling, N., Weinhold, E., and Saenger, W. (1997) *J. Mol. Biol. 265*, 56−67.
42. Nicholls, A., Sharp, K. A., and Honig, B. (1991) *Proteins 11*, 281−296.

BI034026P